

Electronic Supporting Information

A stable luminescent anionic porous metal-organic framework for moderate adsorption of CO₂ and selective detection of nitro explosives

En-Long Zhou, Peng Huang, Chao Qin,* Kui-Zhan Shao, Zhong-Min Su*

Experimental Section

Materials and Instrumentation: All chemicals were obtained commercially and used without additional purification. Single-crystal diffraction was conducted on a Bruker Smart Apex CCD II area-detector diffractometer with graphite-monochromated Mo $K\alpha$ radiation ($\lambda = 0.71073 \text{ \AA}$) at room temperature. Elemental analyses (C, H, and N) were performed on a Perkin-Elmer 2400 CHN elemental analyzer and the rare earth metal contents were determined with a PLASMA-SPEC(I) ICP atomic emission spectrometer. IR spectra were recorded in the range $4000\text{-}400 \text{ cm}^{-1}$ on Mattson Alpha-Centauri spectrometer using KBr pellets. Thermal gravimetric (TG) analyses were performed on a Perkin-Elmer TGA7 instrument in flowing N_2 with a heating rate of $10 \text{ }^\circ\text{C}/\text{min}$. Powder X-ray diffraction (XRD) measurements were performed on a Rigaku D/MAX-3 instrument with Cu $K\alpha$ radiation in the angular range $2\theta = 3^\circ\text{-}50^\circ$ at 293 K . Gas adsorption measurement was measured with Quantachrome Autosorb-iQ. UV-vis absorption spectra were recorded on Hitachi U3030 spectrometer. The emission spectra were recorded using the F-4500 FL spectrophotometer.

Synthesis of $[(\text{CH}_3)_2\text{NH}_2]_3[\text{Zn}_4\text{Na}(\text{BPTC})_3]\cdot 4\text{CH}_3\text{OH}\cdot 2\text{DMF}$ (1): A mixture of sodium biphenyl-3,3',5,5'-tetracarboxylate (Na_4BPTC , 42mg, 0.1 mmol) and ZnCl_2 (27 mg, 0.2 mmol) were dissolved in 3 mL N,N-dimethylformamide (DMF) and 3 mL methanol (MeOH) and stirred

for 10 minutes. Then the mixture was transferred into and sealed in a Teflon reactor (18 mL) and heated at 100 °C for 72 h. Colorless block crystals of the product were formed and collected by filtration and washed with DMF several times after the mixture was cooled to room temperature. Yield: 40 mg (~93.8% based on H₄BPTC). Elemental analysis for C₆₄H₇₂O₃₀N₅NaZn₄ (%): calcd. H: 4.33 C: 45.86 N: 4.18%. found: 4.12 C: 46.02 N: 4.27%.

X-ray Crystallography: Single-crystal diffractometry was conducted on a Bruker Smart Apex CCD II area-detector diffractometer with graphite-monochromated Mo K_{α} radiation ($\lambda = 0.71073 \text{ \AA}$) at room temperature. The linear absorption coefficients, scattering factors for the atoms, and anomalous dispersion corrections were taken from the International Tables for X-Ray Crystallography. Empirical absorption corrections were applied. The structures were solved by using the direct method and refined through the full-matrix least-squares method on F₂ using SHELXS-97. The total interstitial solvent molecule contents were determined by TGA.

Crystal data of **1**: Monoclinic, $a = 12.285(5) \text{ \AA}$, $b = 31.023(5) \text{ \AA}$, $c = 22.686 \text{ \AA}$, $V = 8623(4) \text{ \AA}^3$, $T = 298(2) \text{ K}$, space group $C2/c$, $Z = 4$, 18663 reflections measured, 5944 independent reflections ($R_{\text{int}} = 0.0530$). The final R_1 values were 0.0938 ($I > 2\sigma(I)$). The final $wR(F^2)$ values were 0.1312 ($I > 2\sigma(I)$). The goodness of fit on F^2 was 0.8650.

Small solvent molecule sensing experiments: The activated and fine grinding sample of **1a** (3 mg) was immersed in different pure organic solvents (3 mL). Then the sample was treated by ultrasonication for 3 h and then aged for 2 days to form a stable emulsion before the fluorescence study.

Aromatic compounds sensing experiments: The activated and fine grinding sample of **1a** (2 mg) was immersed in DMF (3 mL), treated by ultrasonication for 30 min. Then equal volume (80 μ L) of aromatic molecules was added into the above samples. Finally, stable emulsion was formed by ultrasonication for additional 3 h and then aged for 2 days before the fluorescence study. The aromatic compounds are benzene (Bz), toluene (TO), nitrobenzene (NB), chlorobenzene (CB), o-xylene (OX), p-xylene (PX), m-xylene (MX) and styrene (ST).

Nitro compounds sensing experiments: In typical experimental setup, 2 mg of **1a** is weighed and dispersed in 2 mL DMF, treated by ultrasonication for 3 h and aged for 2 days to form stable emulsion. The fluorescence of emulsion upon excitation at 295 nm was measured in-situ after incremental addition of freshly prepared analyte solutions (1mM).

Gas adsorption experiments: The N₂ and CO₂ sorption measurements were performed on an automatic volumetric adsorption equipment (Quantachrome Autosorb-iQ). Before gas adsorption measurements, the sample was immersed in dichloromethane for 24 h, and the extract was

decanted. Fresh dichloromethane was subsequently added, and the crystals were allowed to stay for an additional 24 h to remove the methonal solvates. After the removal of dichloromethane by decanting, the sample was activated by drying under a dynamic vacuum at 373 K overnight. Before the measurement, the sample was dried again by using the 'outgas' function of the surface area analyzer for 12 h at 373 K.

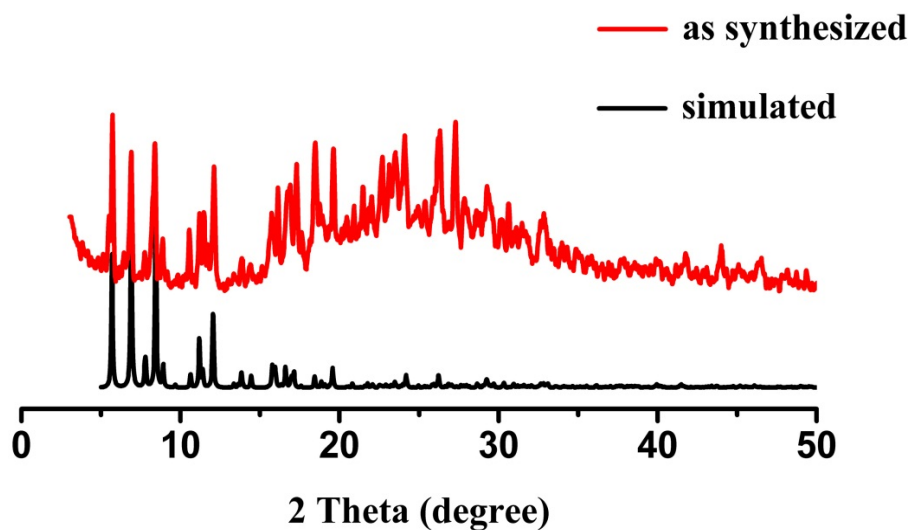


Fig. S1 PXRD patterns of the simulated one and as synthesized sample.

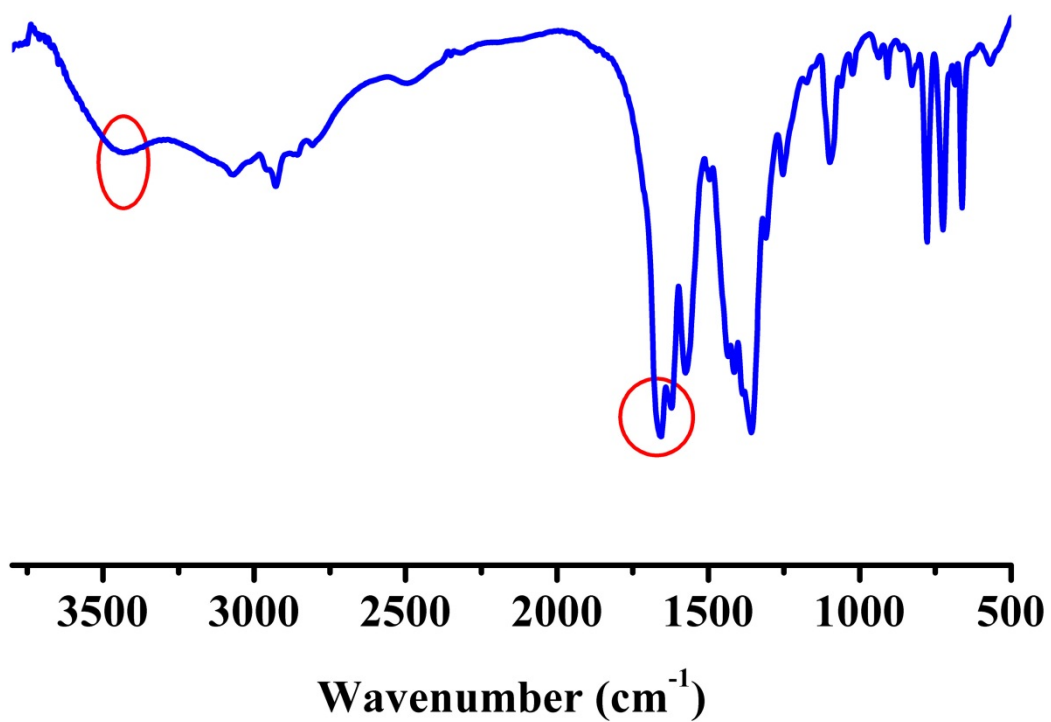


Fig. S2 The IR spectroscopy of compound 1.

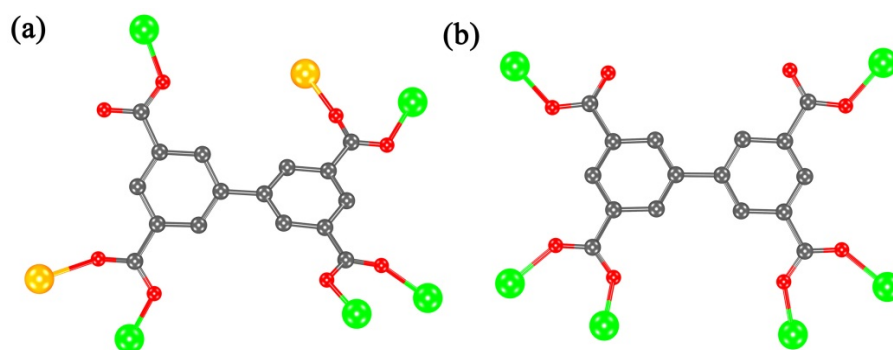


Fig S3. The two type of coordination codes of BPTC ligand in compound **1**.

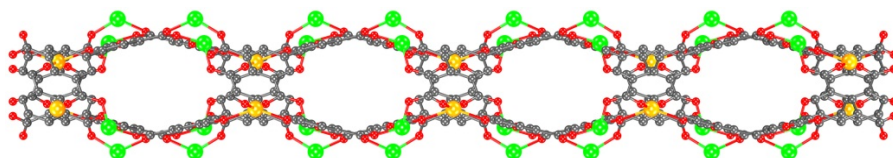


Figure S4. The small 1D hexagonal channel in the the 2D sheet viewed along the crystallographic c axis.

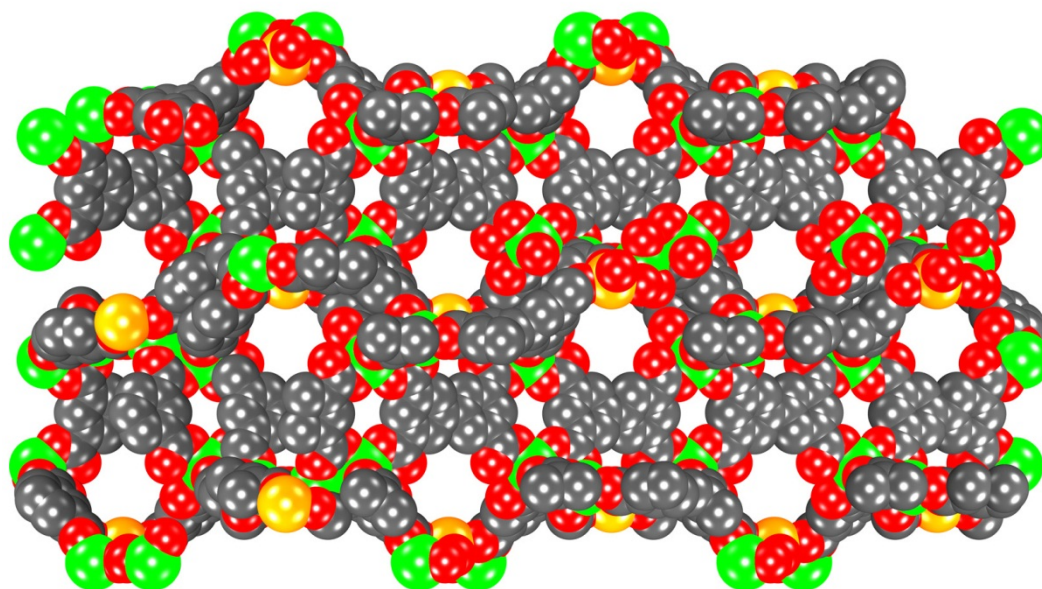


Figure S5. The 3D structure viewed along the a axis

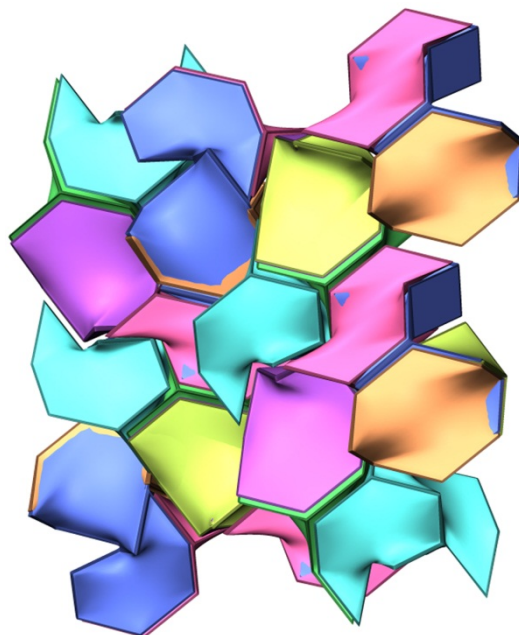


Figure S6. The natural tiling of compound 1.

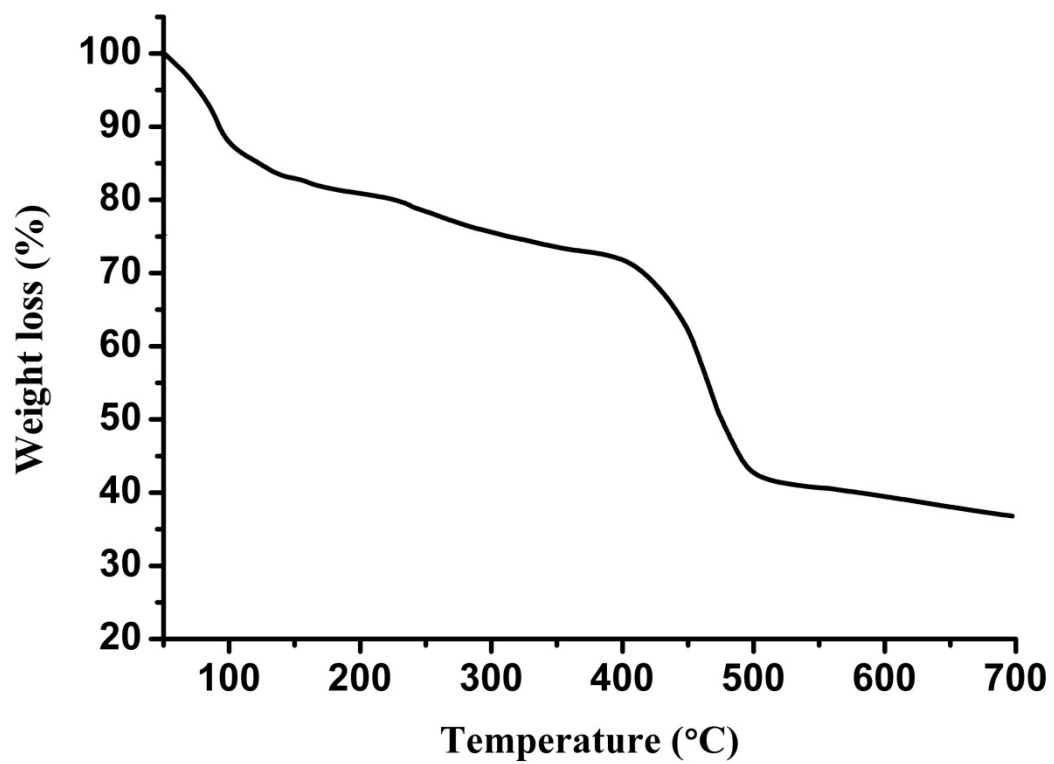


Figure S7. The TG curve of compound 1.

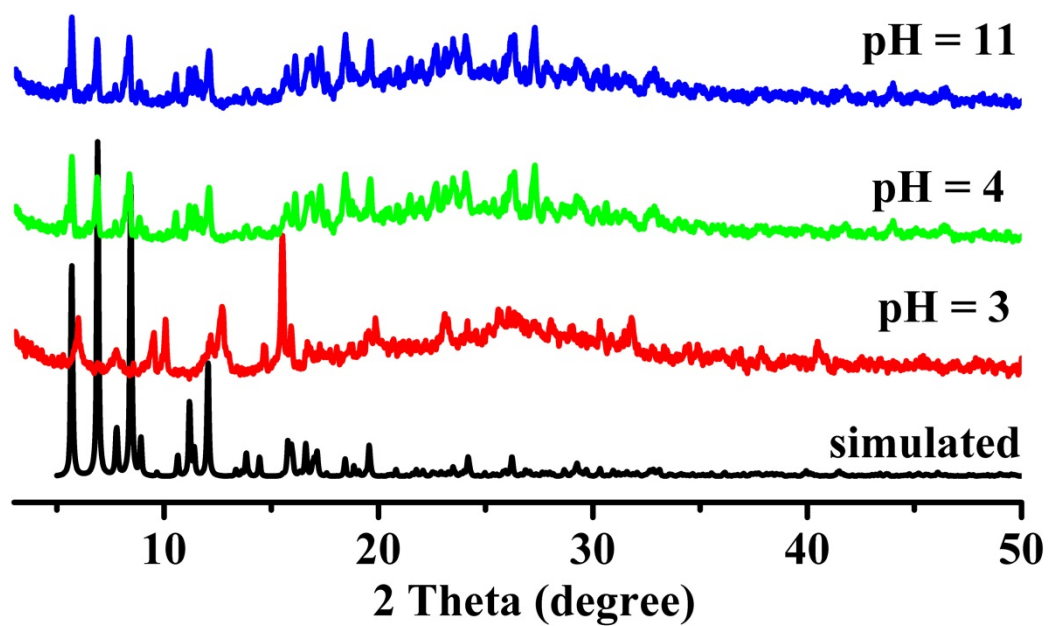


Figure S8. The XRD patterns of compound **1** in the solution of different pH.

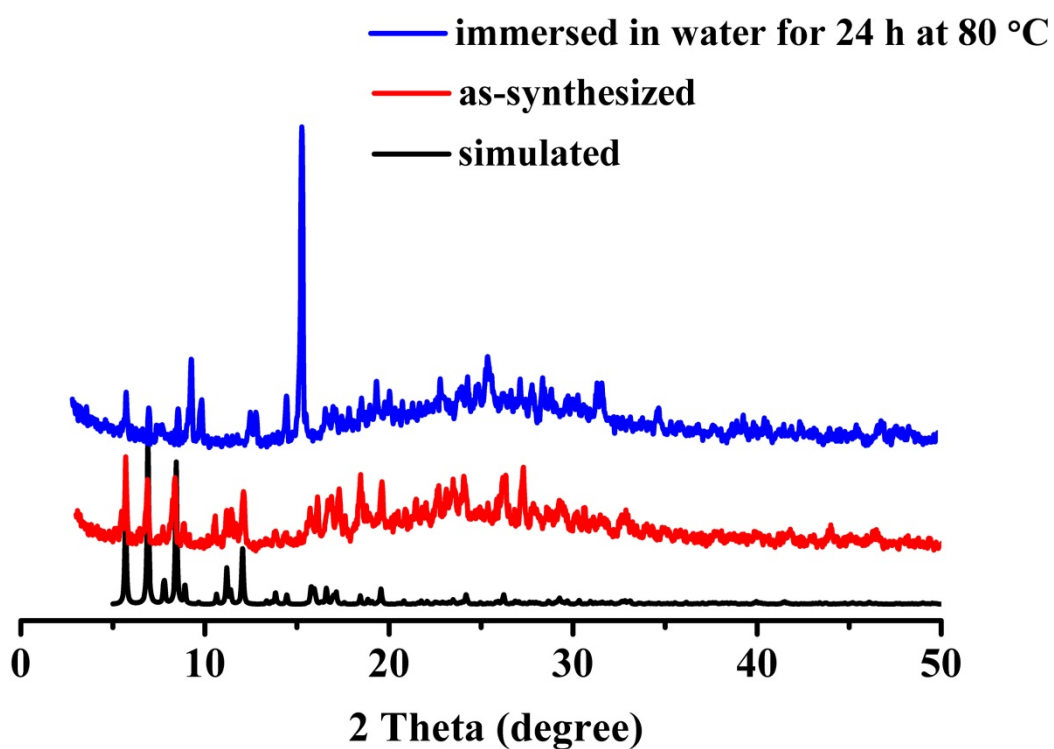


Fig S9. The PXRD patterns of compound **1** immersed in water at 80 °C

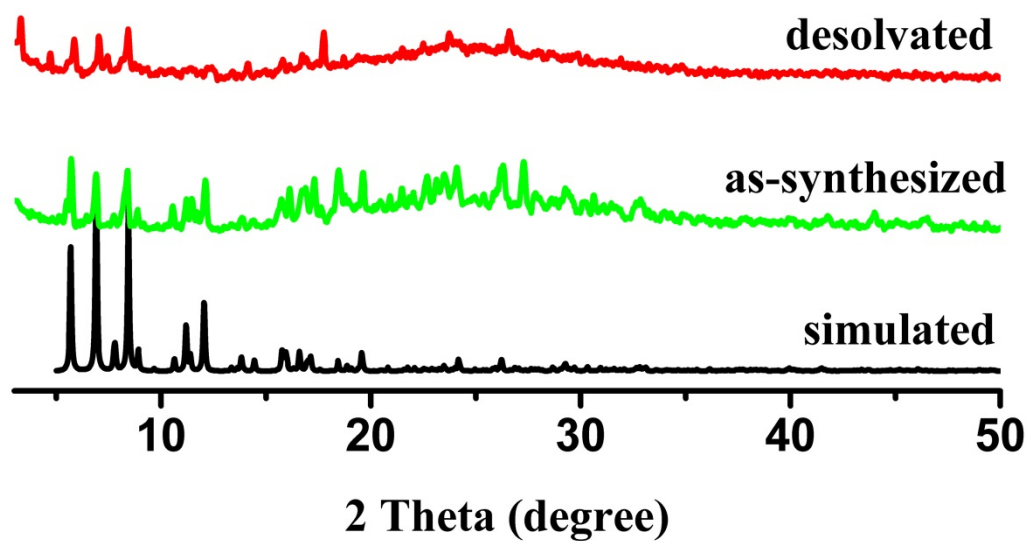


Fig S10. The XRD patterns of simulated, as synthesized and desolvated **1 (1a)**.

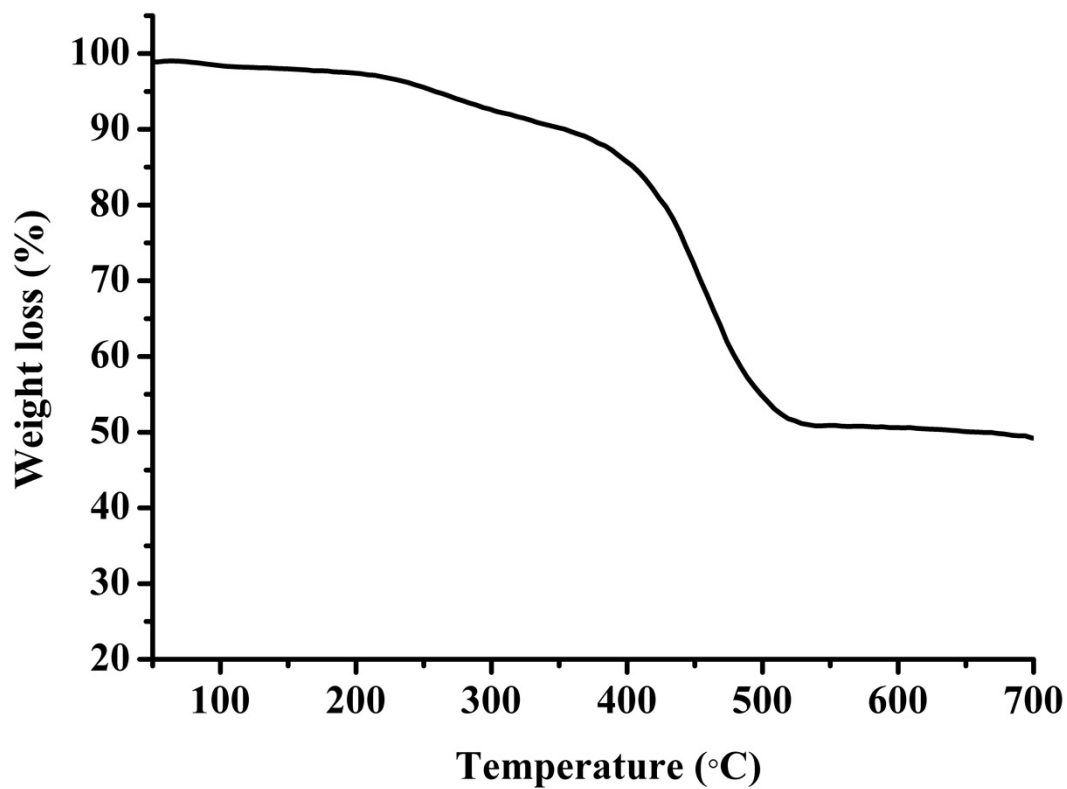


Fig S11. The TG curve of desolvated compound **1 (1a)**.

Table S1. The relevant data of CO₂ adsorption capacities for MOFs at 273 K

Compound	Surface area (m ² /g)		capacity (wt%)	pressure (bar)	ref
	Langmuir	BET			
Compound 1	1002	865	17.1	1	This work
Mg/DOBDC	1905	1495	35.2	1	<i>Proc. Natl. Acad. Sci. U.S.A.</i> , 2009 , 106, 20637
SIFSIX-2-Cu-i	821	735	28.6	1	<i>Nature</i> , 2013 , 495, 80
MAF-35	1043	974	25.3	1	<i>Chem. Commun.</i> 2013 , 49, 11728
NTU-111		2450	24.8	1	<i>Chem. Commun.</i> 2014 , 50, 4683
Zn ₂ (Atz) ₂ (ox)			19.1	1.2	<i>Science</i> , 2010 , 330, 650
Co ₉ (int) ₁₈ (μ ₂ -OH ₂) ₄ (H ₂ O) ₂	835	600	16.7	1	<i>CrystEngComm</i> , 2014 , 16, 4088-4090.
NJU-Bai8	1196	1103	12.8	1	<i>J. Am. Chem. Soc.</i> 2013 , 135, 562
ROD-6	535	345	11.6	1	<i>Chem. Commun.</i> 2014 , 50, 4047
IFMC-69	664	581	11.0	1	<i>Chem. Sci.</i> , 2014 , 5, 1368
ZIF-301	825	680	10.4	1	<i>Angew. Chem. Int. Ed.</i> 2014 , 53, 10645
[Cu(bcppm)H ₂ O]		155	8.14	1	<i>J. Am. Chem. Soc.</i> 2013 , 135, 10441
JLU-Liu4			7.8	1	<i>Cryst. Growth Des.</i> , 2014 , 14, 2375
ZIF-100	780	595	7.48	1	<i>Nature</i> . 2008 , 453, 207

Table 2. The relevant data of CO₂ adsorption capacities for MOFs at 298 K

Compound	Surface area (m ² /g)		capacity (wt%)	pressure (bar)	ref
	Langmuir	BET			
Compound 1	1002	865	9.4	1	This work

SIFSIX-2-Cu-i	821	735	23.8	1	<i>Nature</i> , 2013 , 495, 80
MAF-35	1043	974	19.6	1	<i>Chem. Commun.</i> 2013 , 49, 11728
Mg₂(dobpdc)			16.5		<i>J. Am. Chem. Soc.</i> 2012 , 134, 7056
Cu-BTTri	1900	1770	14.3	1	<i>J. Am. Chem. Soc.</i> , 2009 , 131, 8784
NTU-111		2450	13.3	1	<i>Chem. Commun.</i> 2014 , 50, 4683-4685
Co₉(int)₁₈(μ₂-OH₂)₄(H₂O)₂	835	600	11.5	1	<i>CrystEngComm</i> , 2014 , 16, 4088-4090.
NJU-Bai8	1196	1103	11.2	1	<i>J. Am. Chem. Soc.</i> 2013 , 135, 562–565
[Cu(bcppm)H₂O]		155	7.48	1	<i>J. Am. Chem. Soc.</i> 2013 , 135, 10441
IFMC-69	664	581	7.3	1	<i>Chem. Sci.</i> , 2014 , 5, 1368-1374
ROD-6	535	345	7.73	1	<i>Chem. Commun.</i> 2014 , 50, 4047-4049
ZIF-301	825	680	6.4	1	<i>Angew. Chem. Int. Ed.</i> 2014 , 53, 10645
JLU-Liu4			5.4	1	<i>Cryst. Growth Des.</i> , 2014 , 14, 2375–2380

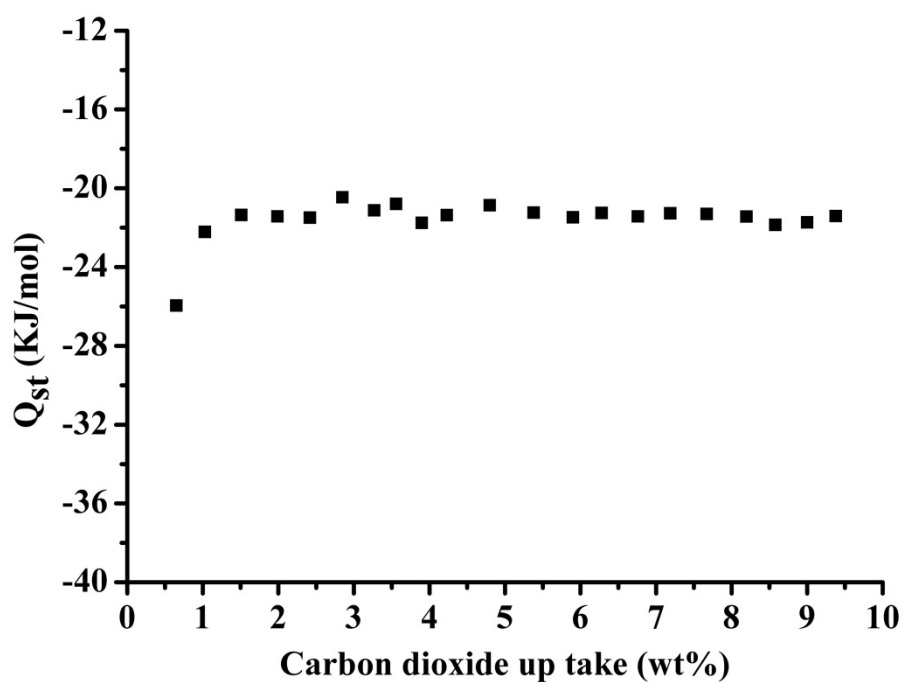


Fig S12. The CO₂ isosteric adsorption enthalpies calculated by Clausius–Clapeyron

equation between isotherms at 273 and 298 K.

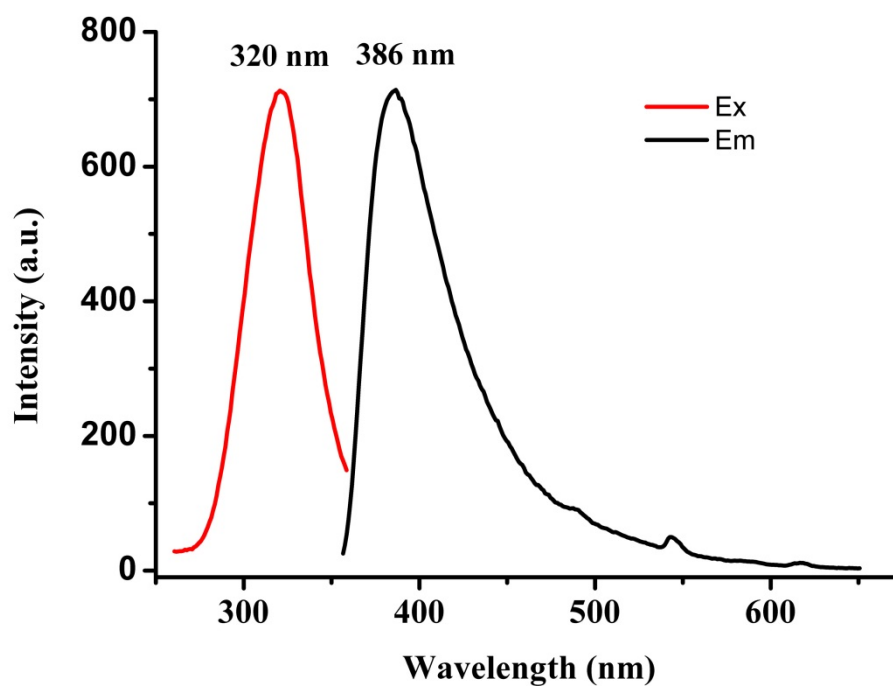


Fig S13. The excitation and emission spectra of BPTC.

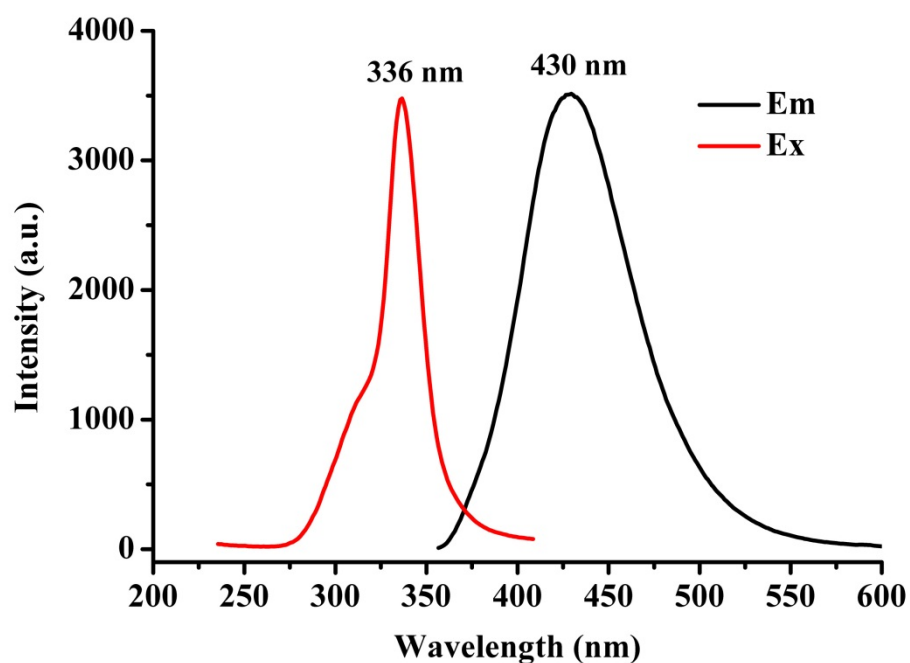


Fig S14. The excitation and emission spectra of compound 1.

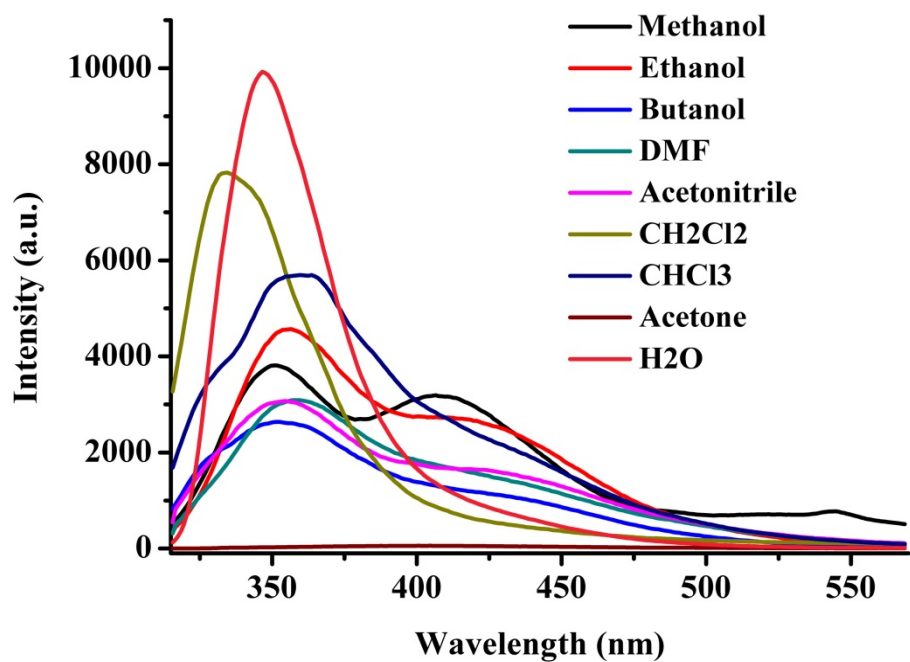


Fig S15. The PL spectra of **1a** that were immersed in different small solvents.

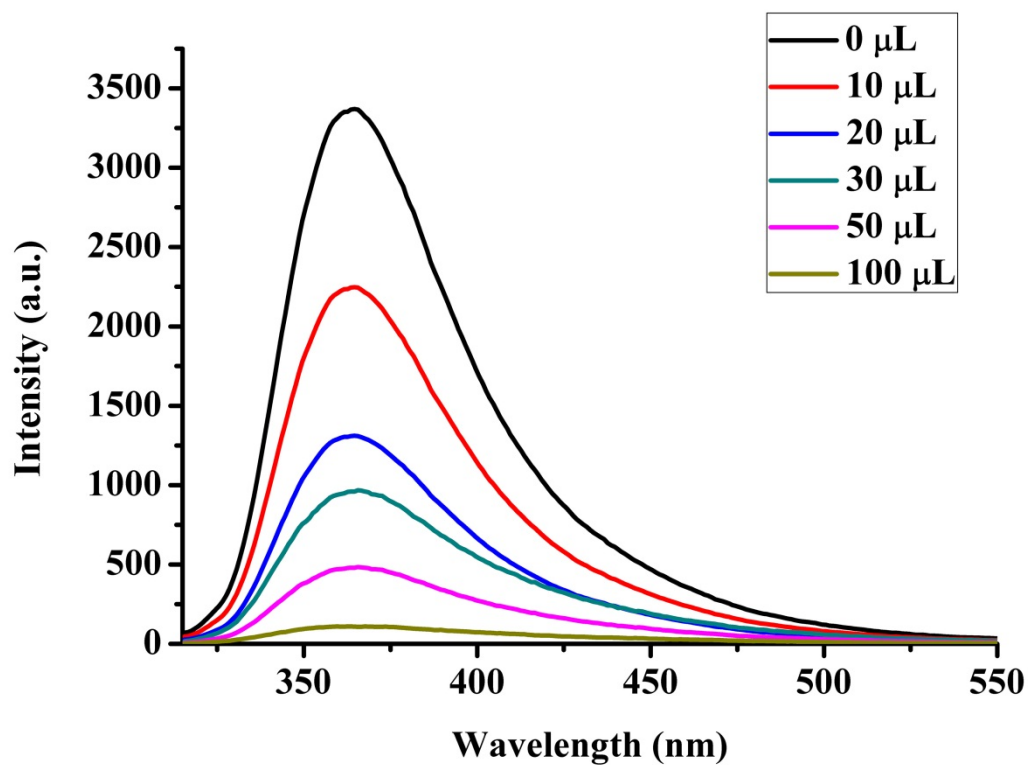


Fig S16. The PL spectra of **1a** upon incremental addition of acetone to **1a** dispersed in DMF.

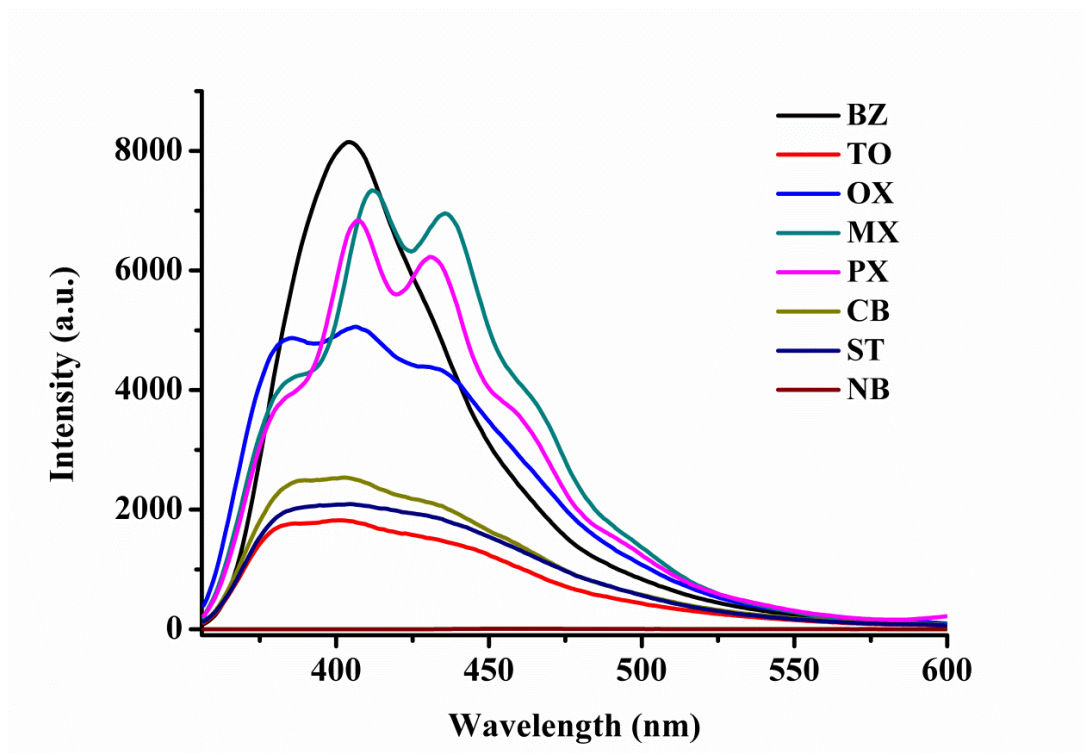


Fig S17. The PL spectra of **1a** that were immersed in different aromatic compounds.

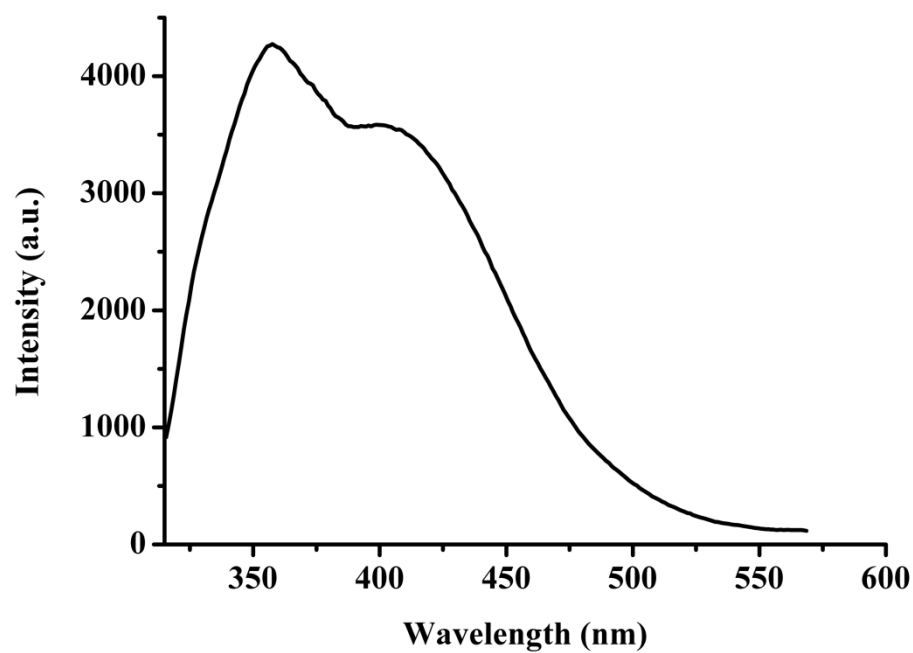


Fig S18. The emission spectra of compound **1a** immersed in DMF.

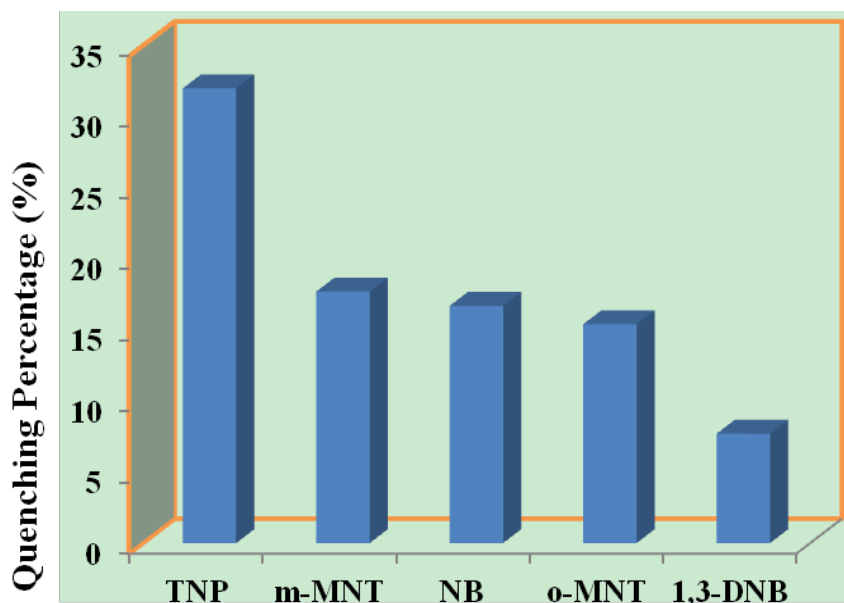


Fig S19. Quenching percentage upon addition of different 10 μL nitro explosives (1mM)

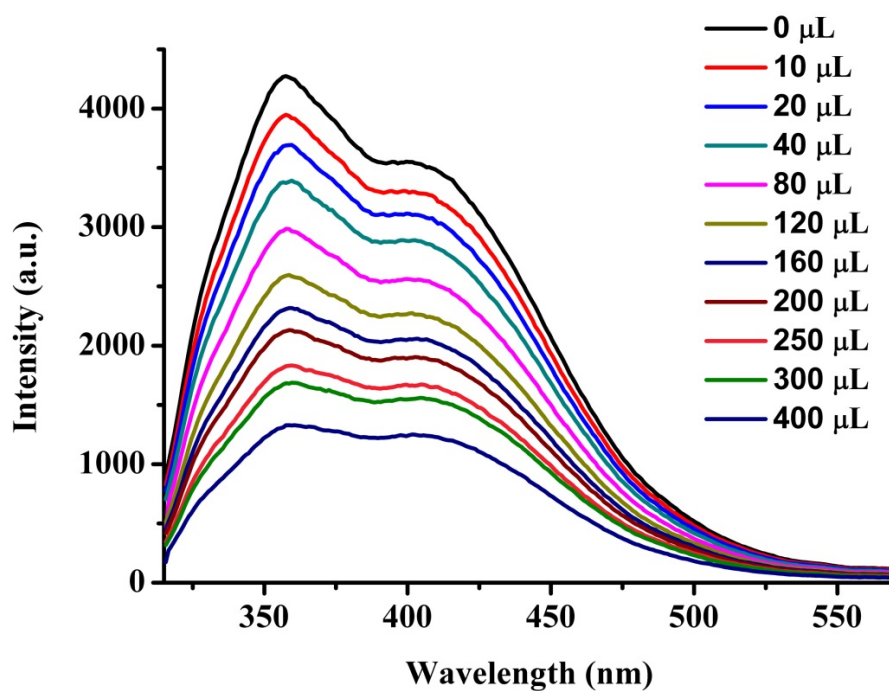


Fig. S20 Emission spectra of compound **1a** dispersed in DMF upon incremental addition of 1,3-DNB solution (1mM) in DMF.

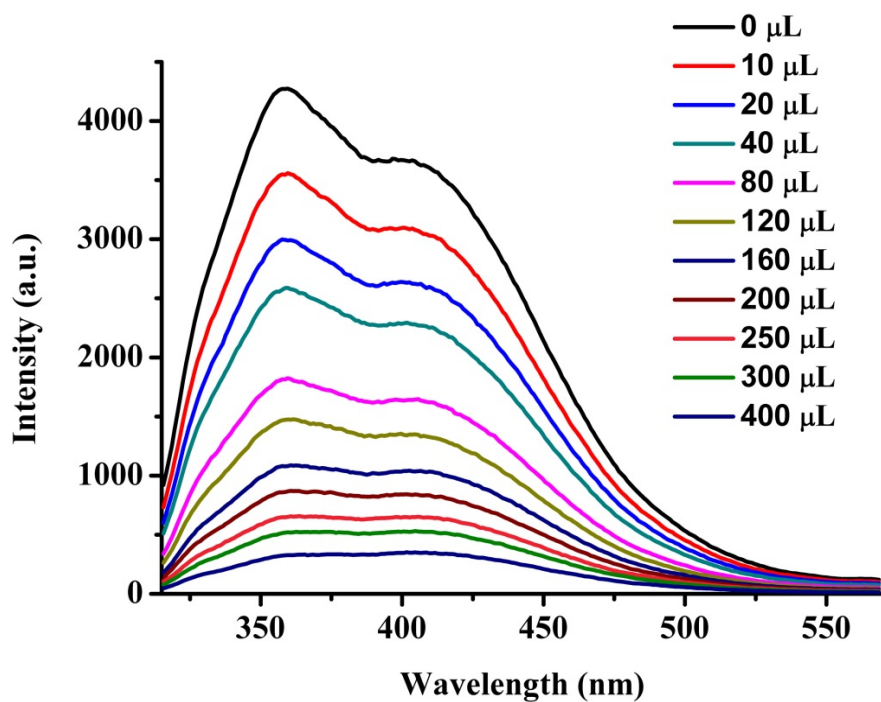


Fig. S21 Emission spectra of compound **1a** dispersed in DMF upon incremental addition of NB solution (1mM) in DMF.

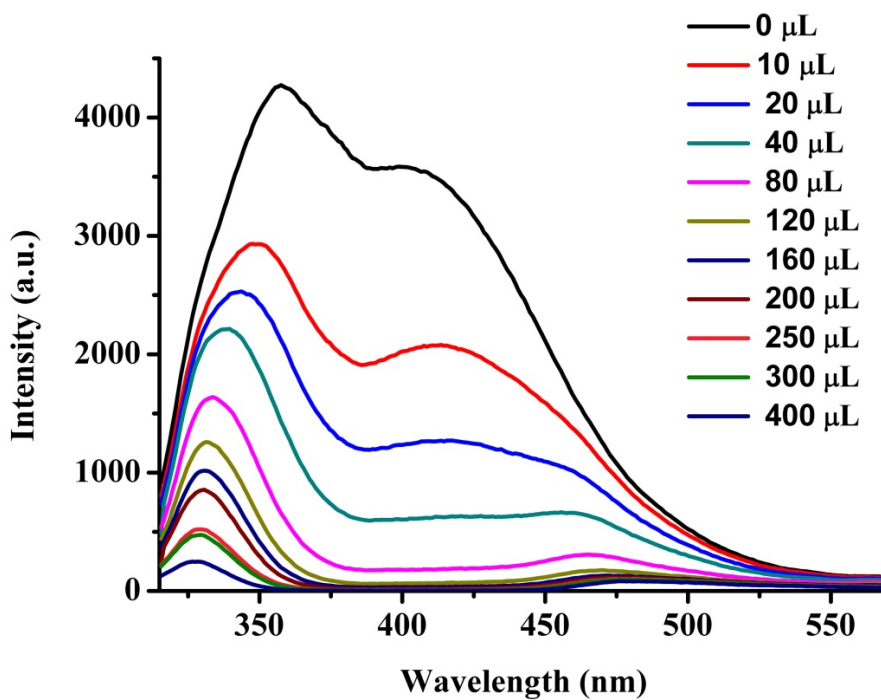


Fig. S22 Emission spectra of compound **1a** dispersed in DMF upon incremental addition of TNP solution (1mM) in DMF.

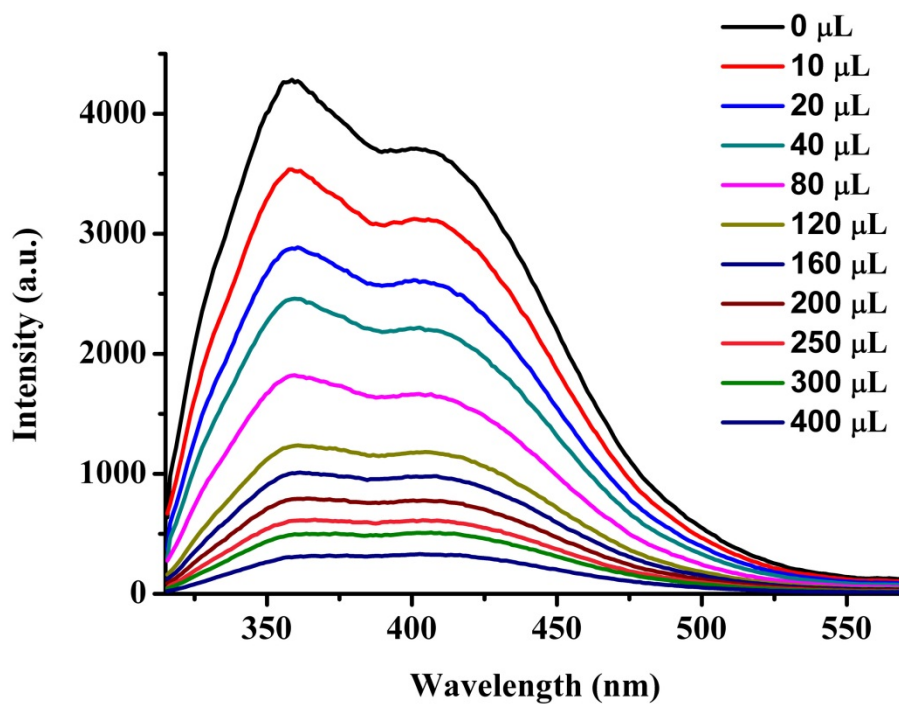


Fig. S23 Emission spectra of compound **1a** dispersed in DMF upon incremental addition of *m*-MNT solution (1mM) in DMF.

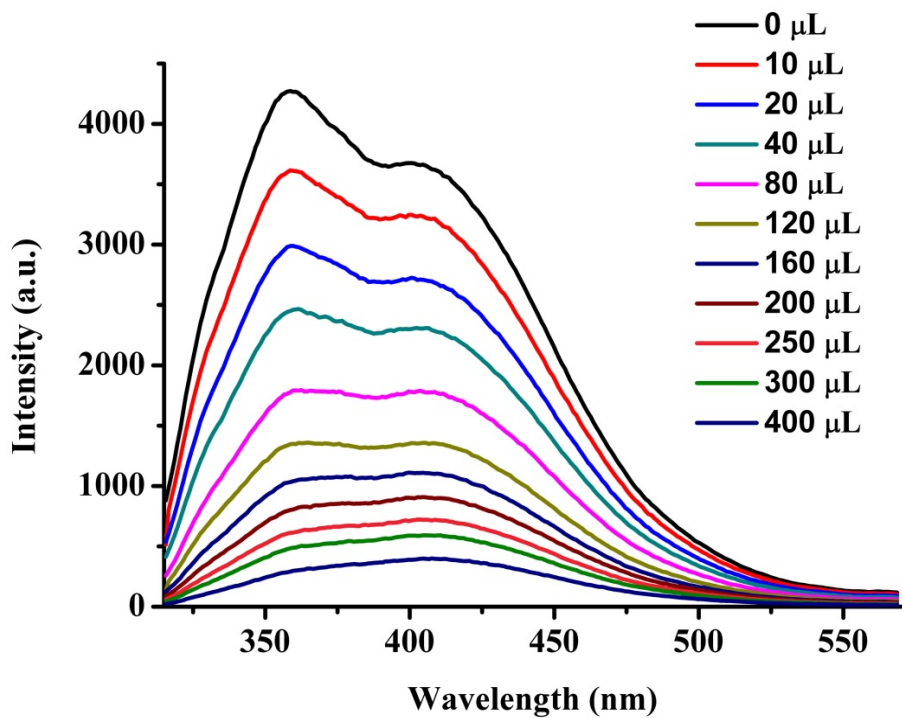


Fig. S24 Emission spectra of compound **1a** dispersed in DMF upon incremental addition of *o*-MNT solution (1mM) in DMF.

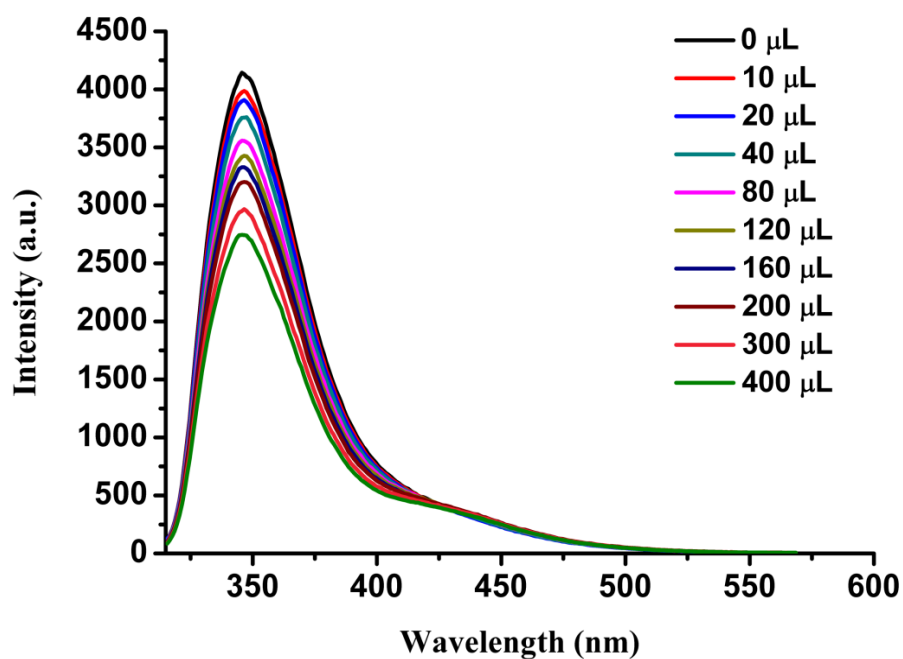


Fig. S25 Emission spectra of compound **1a** dispersed in water upon incremental addition of 1,3-DNB solution (1mM) in DMF.

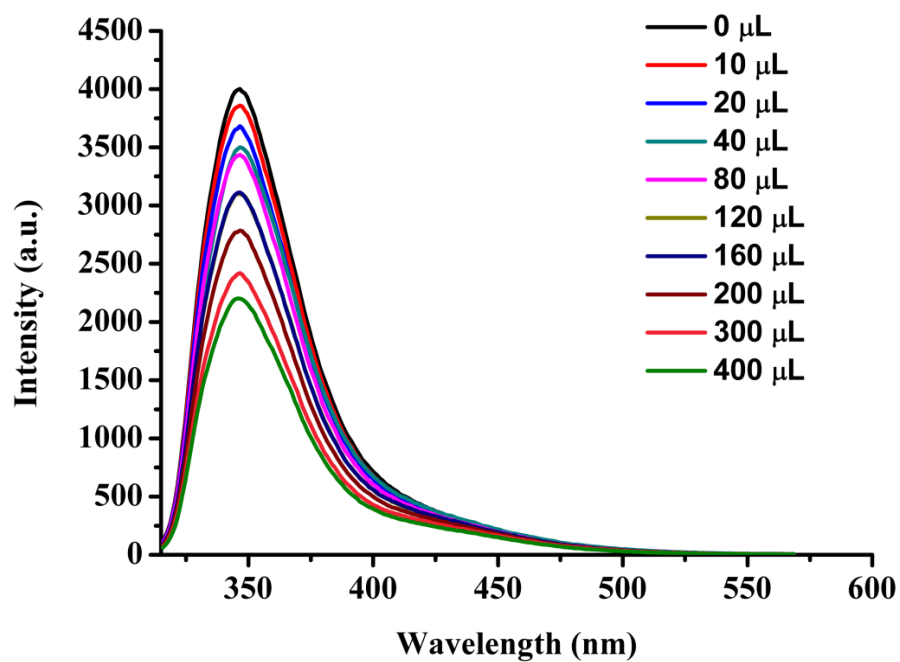


Fig. S26 Emission spectra of compound **1a** dispersed in water upon incremental addition of NB solution (1mM) in DMF.

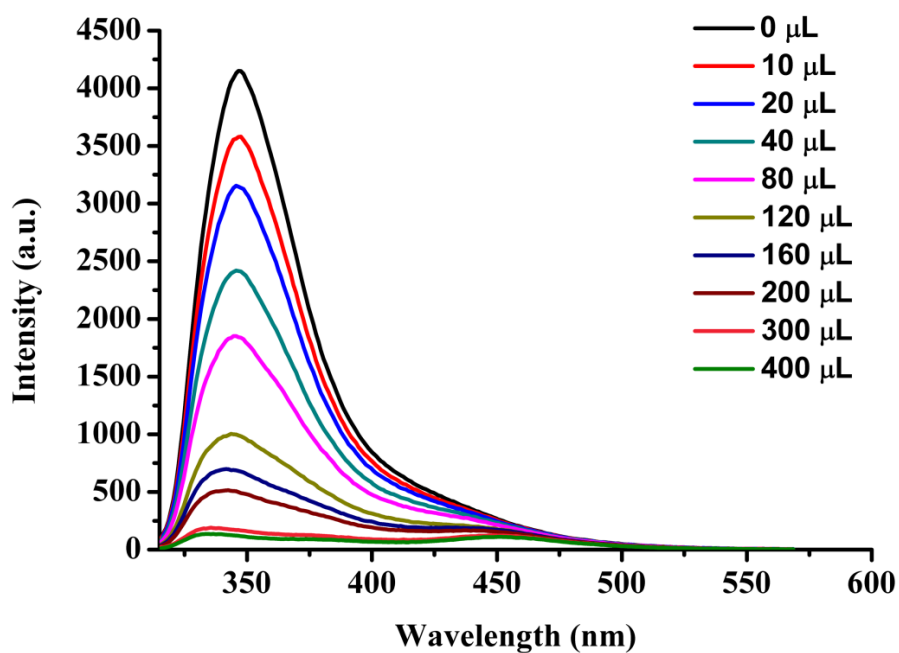


Fig. S27 Emission spectra of compound **1a** dispersed in water upon incremental addition of TNP solution (1mM) in DMF.

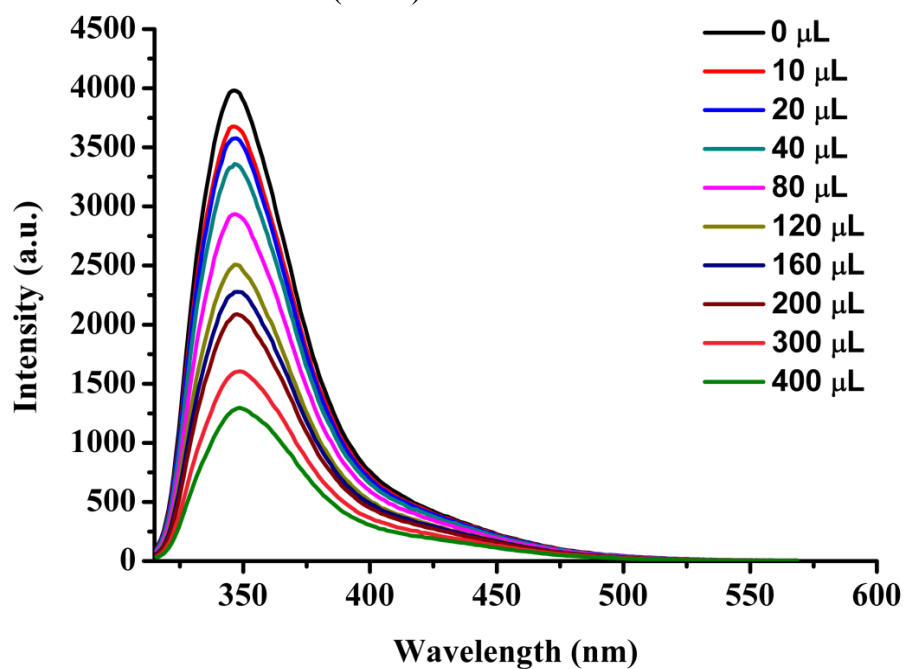


Fig. S28 Emission spectra of compound **1a** dispersed in water upon incremental addition of *m*-MNT solution (1mM) in DMF.

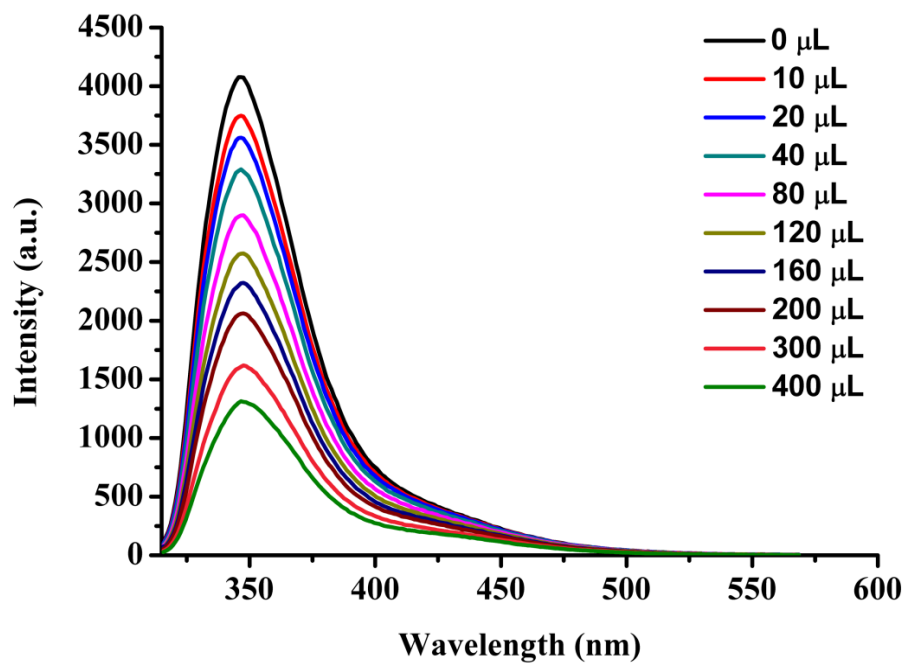


Fig. S29 Emission spectra of compound **1a** dispersed in water upon incremental addition of *o*-MNT solution (1mM) in DMF.

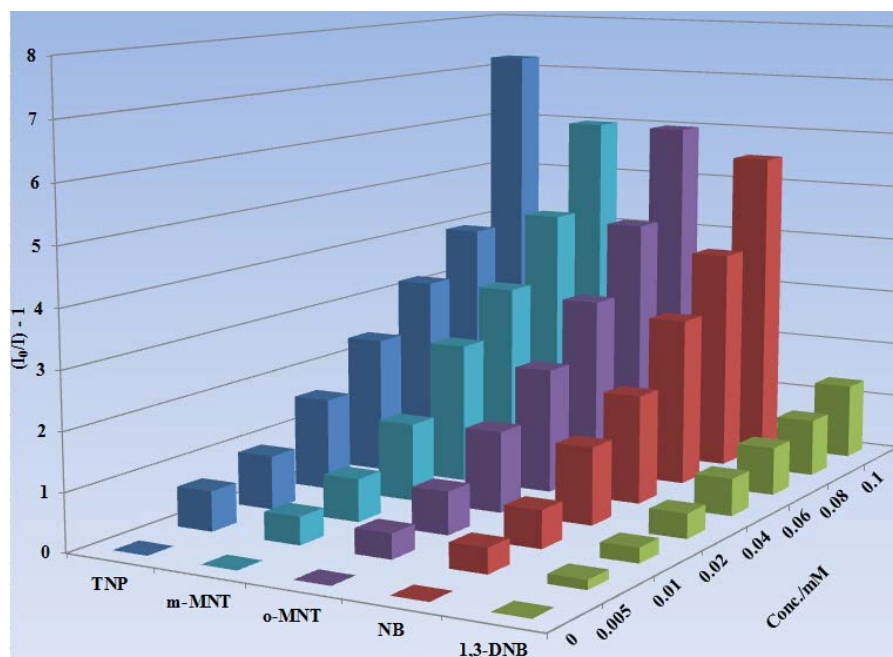


Fig. S30 Corresponding Stern-Volmer plots of $I_0/I-1$ versus analyte concentrations in DMF.

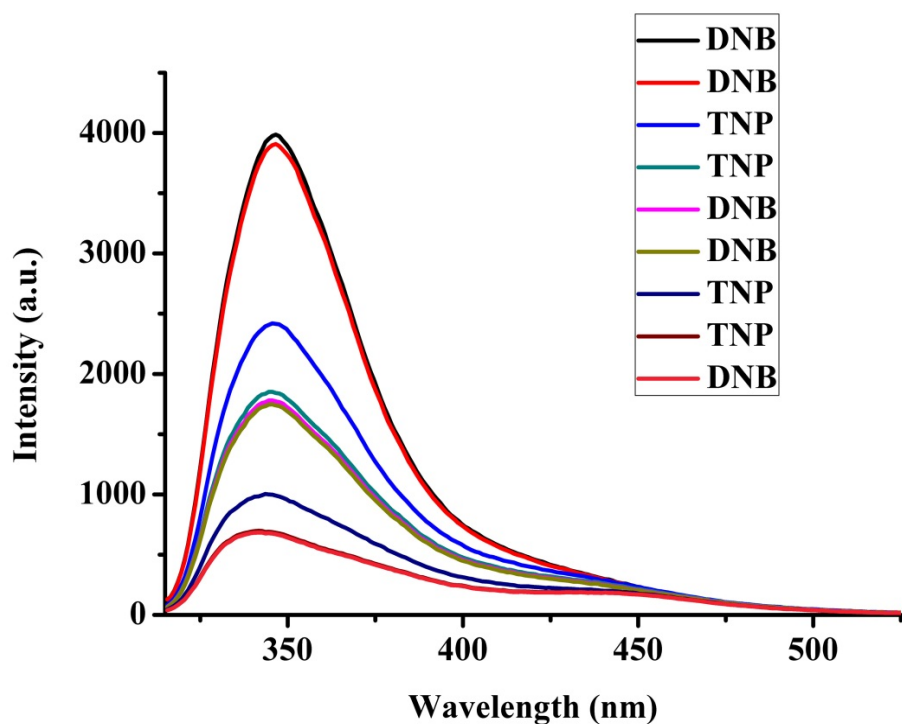


Fig. S31 Emission spectrum of **1a** in water upon addition of DMF solution of DNB followed by TNP (1mM, DNB and TNP 40 μ L addition each time).

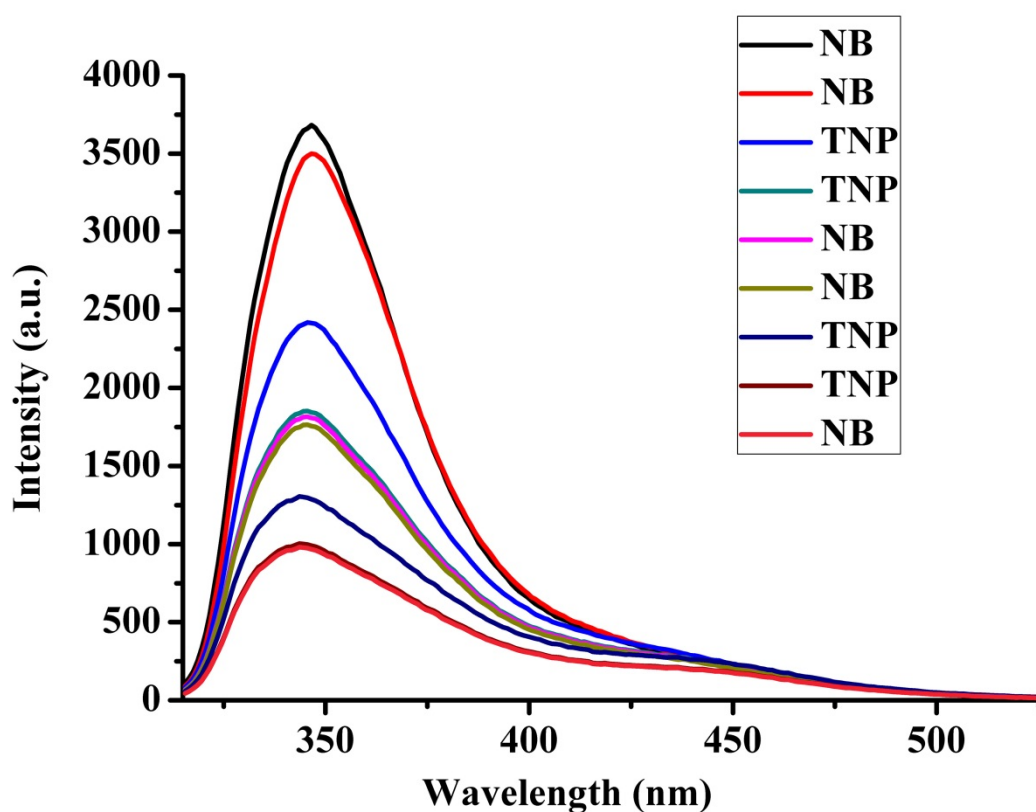


Fig. S32 Emission spectrum of **1a** in water upon addition of DMF solution of NB followed by TNP (1mM, NB and TNP 40 μ L addition each time).

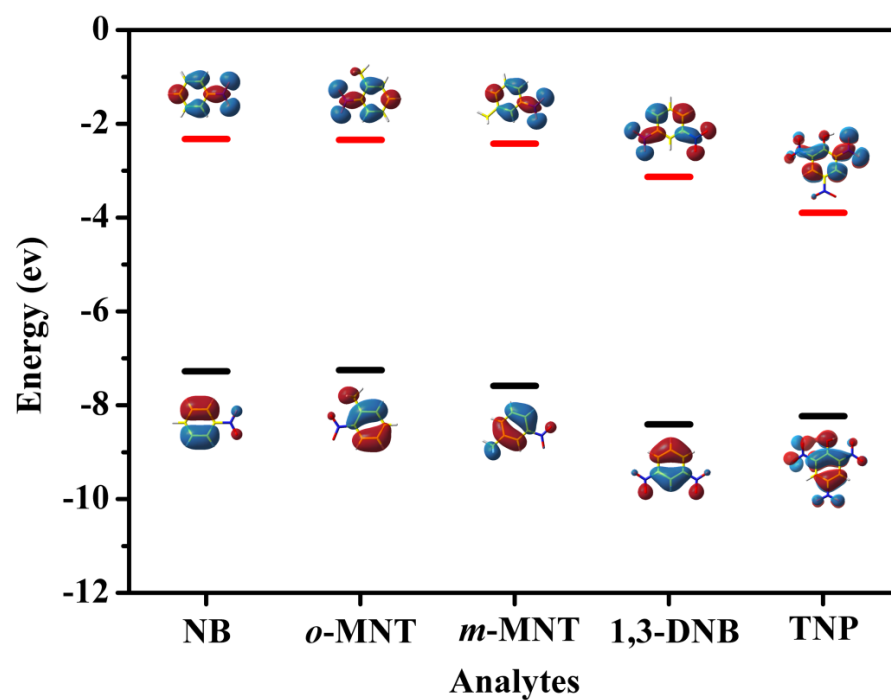


Fig. S33 Shapes of HOMO and LUMO of the molecular orbitals considered and the relative energy level investigated by the B3LYP/6-31G** method.

Table S3: HOMO and LUMO energies calculated for explosive analytes (at B3LYP/6-31G* level of theory).

Analytes	HOMO (eV)	LUMO (eV)	Band gap (eV)
NB	-7.587	-2.425	5.162
<i>o</i> -MNT	-7.278	-2.323	4.955
<i>m</i> -MNT	-7.253	-2.347	4.906
1,3-DNB	-8.409	-3.133	5.276
TNP	-8.234	-3.896	4.338

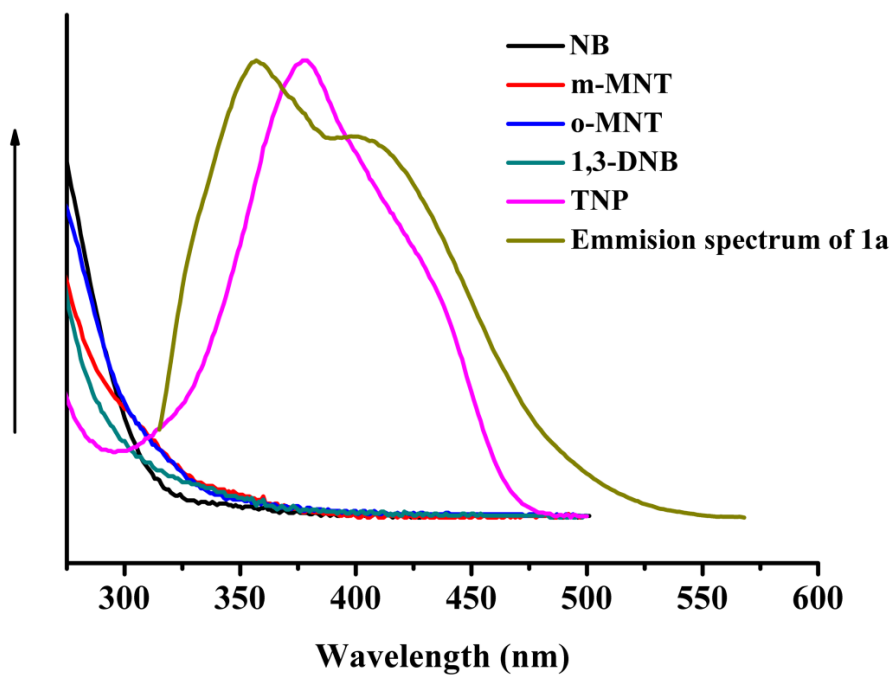


Fig. S34 Spectral overlap between the absorption spectra of analytes and the emission spectrum of **1a** in DMF.